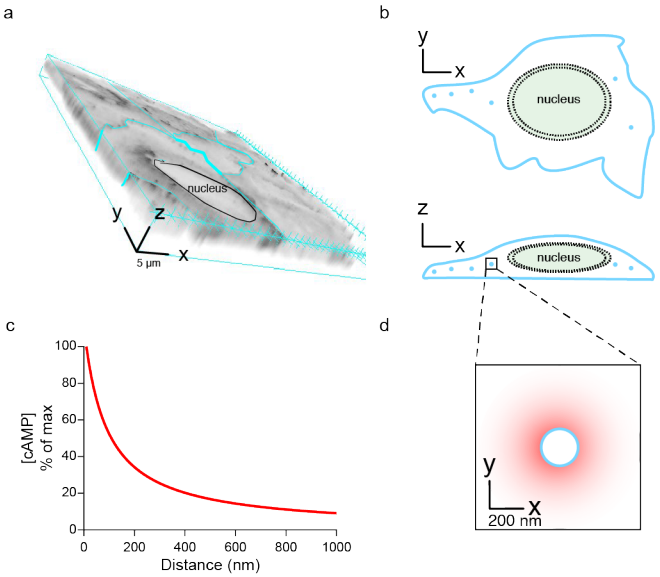

Supplementary Figure 1. Explicit statement of the problem. In order for cAMP production from endosomes to communicate signaling to the nucleus based on location, rather than by generating a sustained elevation of global cytoplasmic cAMP concentration, the concentration gradient resulting from local cAMP production must be communicated spatially downstream. This is problematic because the distance scale of local concentration gradients is inherently shorter than the typical distance between endosomes and the nucleus. **a**, 3D projection of a HEK293 cell monolayer for perspective, highlighting the plasma membrane and endosomes using the membrane adenylyl cyclase isoform 9 (ADCY9) that is present in both compartments. **b**, Schematic of this distribution in xy and xz projections, with endosomes drawn to scale relative to the overall cellular size. **c**, The local cAMP concentration gradient as a function of distance, as predicted by Fick's law at steady state ($\nabla^2 C = \partial C/\partial t = 0$) and assuming spherical symmetry. In this condition, [cAMP] varies inversely with the distance, d, from the surface of the endosome of radius, r, as r / (d + r). Plotted is this relationship for a spherical endosome 200 nm in diameter (r = 100 nm). **d**, Illustration of the spatial disconnect at a cellular distance scale. The local cAMP gradient falls off two or three orders of magnitude too steeply to reach the nucleus.

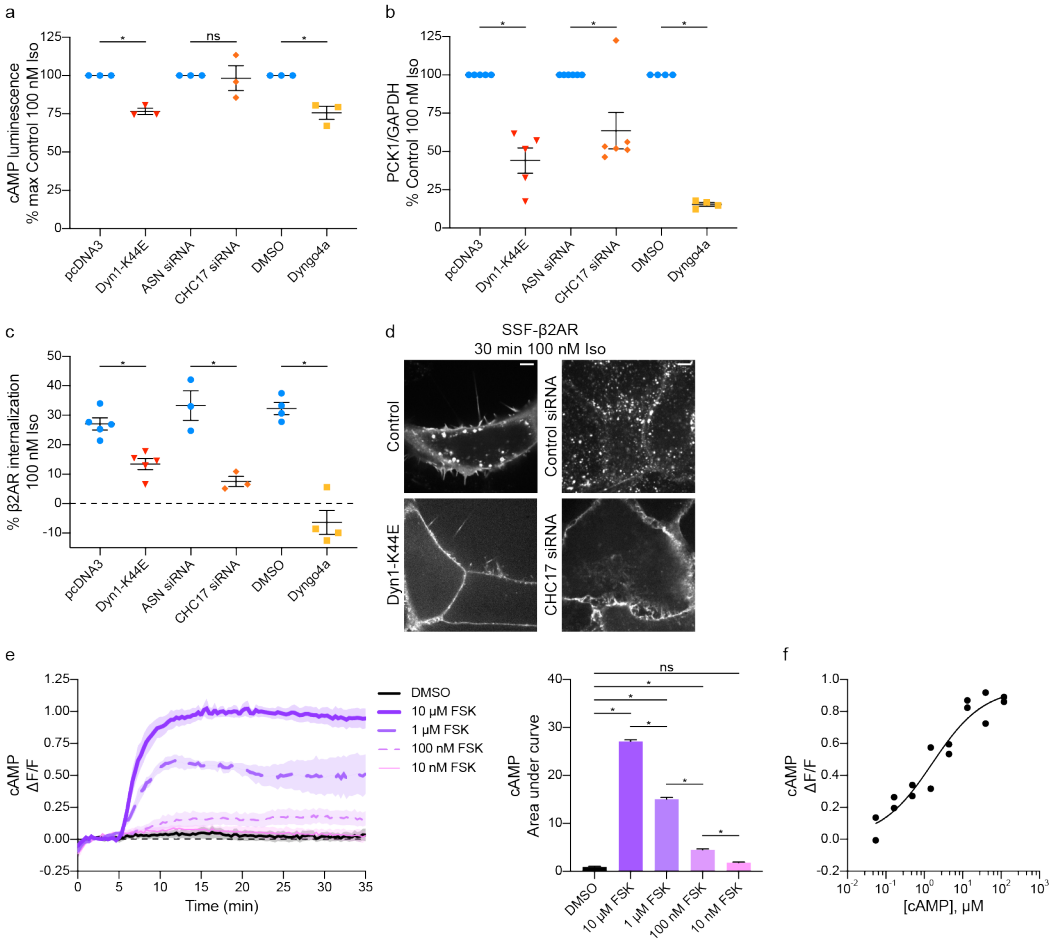

Supplementary Figure 2. Validation and characterization of endocytic blockade methods and GG4B cAMP biosensor. **a-c**, Cells stably expressing cAMP luminescence biosensor (GloSensor-IRES-Rluc) were transiently transfected with pcDNA3 (control) or mCherry-Dyn1-K44E, AllStars Negative (ASN) siRNA (control) or CHC17 siRNA, or pretreated with DMSO (control) and 30 μM Dyngo4a for 15 minutes. **a**, Effects of endocytic blockade on peak cAMP luminescence. The peak luminescence value normalized to the corresponding control Iso condition (n = 3, pcDNA3 vs Dyn1-K44E p = 0.0031; ASN vs CHC17 siRNA p = 0.9861; DMSO vs Dyngo4a p = 0.0023; ordinary one-way ANOVA, Sidak's multiple comparisons test). **b**, Endocytic blockade by multiple methods reduces β2AR-stimulated *PCK1* transcription. qRT-PCR was performed on cells untreated or treated with 100 nM Iso for two hours (n = 5, pcDNA3 vs Dyn1-K44E p < 0.0001; n = 6, ASN vs CHC17 siRNA p < 0.0001; n = 4, DMSO vs Dyngo4a p < 0.0001; by ordinary one-way ANOVA, Sidak's multiple comparisons test). **c**, Endocytic blockade effects on β2AR internalization. Three methods of endocytic inhibition are assayed by β2AR internalization. Cells were untreated or treated with 100 nM Iso for 30 minutes (n = 5, pcDNA3 vs Dyn1-K44E, p = 0.0038; n = 3 ASN vs CHC17 siRNA, p < 0.0001; n = 4 DMSO vs Dyngo4a, p < 0.0001 by ordinary one-way ANOVA, Sidak's multiple comparisons test). **d**, Images of endocytic blockade methods on β2AR internalization. Cell surface β2ARs were labeled using M1-FLAG-647. After 30 minutes of 100 nM Iso, cells were imaged by spinning disk confocal microscopy. Images of representative single slices are shown depicting the amount of β2AR internalization after 30 minutes Iso. Scale bars = 5 μm. **e**, GG4B response to multiple concentrations of forskolin. Cells transfected with the GG4B were imaged by spinning disk confocal microscopy and untreated (DMSO) or treated with 10 μM, 1 μM, 100 nM or 10 nM at Fsk 5 minutes. Area under the curve (right) shown for the quantification of the time series (left). (n ≥ 3, cells ≥ 18 per biological replicate; DMSO vs 100 nM Fsk, DMSO vs 1 μM Fsk, DMSO vs 10 μM Fsk, 10 μM Fsk, vs 10 nM Fsk, 10 μM Fsk vs 100 nM Fsk and 10 μM Fsk vs 1 μM Fsk p < 0.0001; DMSO vs 10 nM Fsk p = 0.2406; Sidak's multiple comparisons test, ordinary one-way ANOVA). **f**, GG4B cAMP fluorescence biosensor characterization *in vitro*. Cytoplasmic fraction prepared from HEK293 cells transiently expressing GG4B

was treated with 100 μM IBMX, and different concentrations of cAMP. Fluorescence was recorded and the data were fit to a non-linear regression model (sigmoidal, 4PL). Data are from one independent experiment.

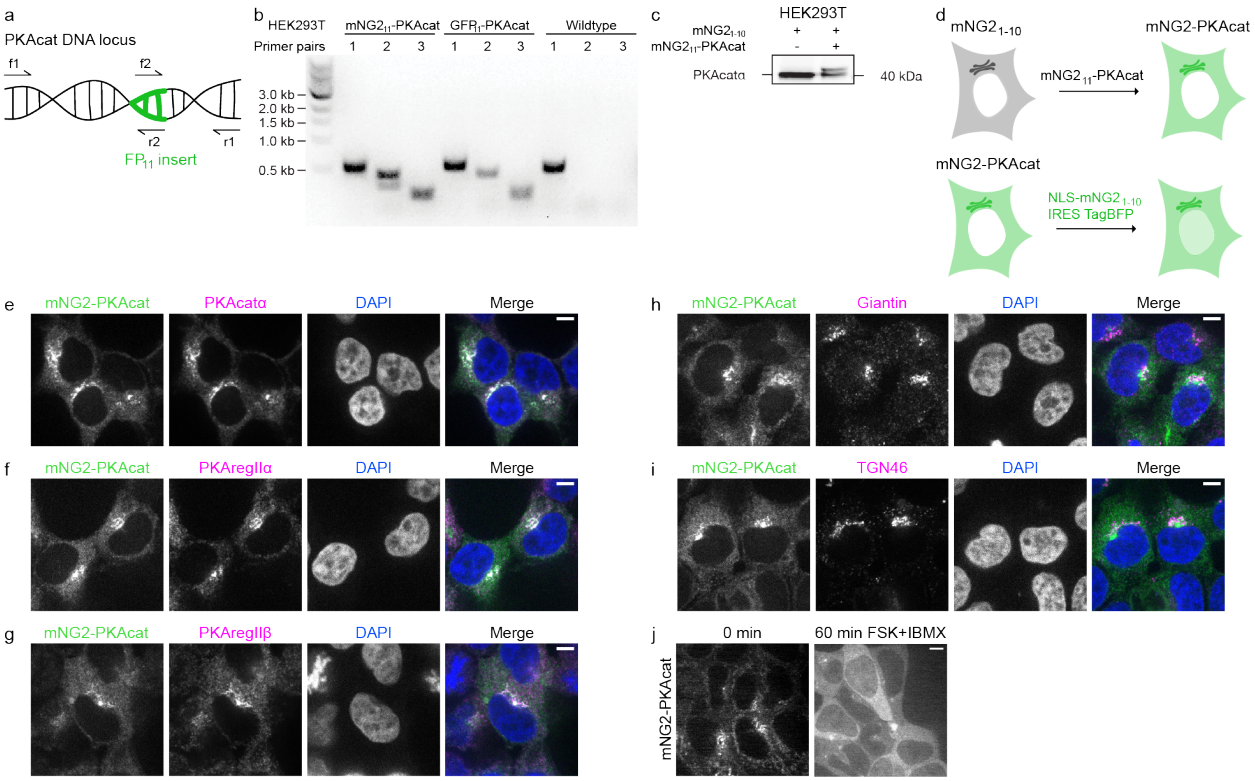

Supplementary Figure 3. Validation and characterization of HEK293T mNG2-PKAcat knock-in line. **a**, Cartoon explaining primer placement for PCR amplified fragments in (**b**). Outer Forward primer (f1), Insert Forward primer (f2), Outer Reverse primer (r1) and Insert Reverse primer (r2). **b**, Gel verifying correct FP_{11} insertion in knock-in cells. Fragments were PCR amplified from extracted genomic DNA. Comparison of PRKACA-mNG2$_{11}$, PRKACA-GFP$_{11}$ and wild type HEK293T cells. Numbers in lanes indicate primer pairs used: [1] primers used f1 and r1, [2] primers used f1 and r2, [3] primers used f2 and r2. **c**, Western blot of cells expressing unlabeled and labeled PKAcat. PKAcat (~42 kDa) was probed in samples from HEK293T cells stably expressing mNG2$_{1-10}$ only or mNG2$_{1-10}$ and mNG2$_{11}$-PKAcat. **d**, Cartoons of mNG2-PKAcat imaging strategies. PKAcat endogenously-tagged with mNG2$_{11}$ in a HEK293T cell line stably expressing mNG2$_{1-10}$ to detect cellular PKAcat (top). Cells co-expressing mNG2$_{1-10}$ and endogenously-tagged mNG2$_{11}$-PKAcat are untransfected or transfected with nuclear localized NLS-mNG2$_{1-10}$ for detection of PKAcat in the nucleus (bottom). **e-i**, Representative images from fixed cell spinning disk confocal microscopy. mNG2-PKAcat cells were fixed and stained for DAPI and PKAcatα (**e**), PKAregIIα (**f**), and PKAregIIβ (**g**), Giantin (**h**), TGN46 (**i**). **j**, Visualizing PKAcat in the nucleus by live imaging. Gene-edited cells expressing endogenous mNG2-PKAcat were untreated or treated with 10 μM Fsk and 500 μM IBMX and imaged after 60 minutes of treatment. Scale bars = 5 μm.

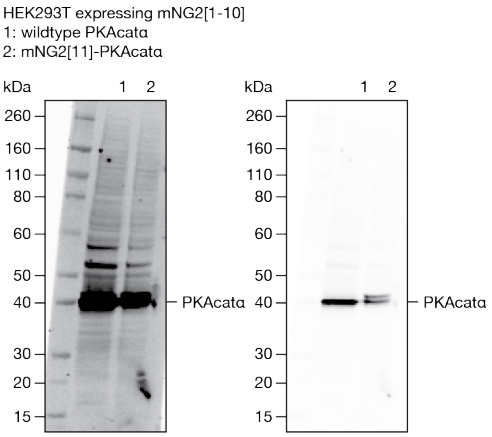

Supplementary Figure 4. Images of the same uncropped blot with different contrasts from Supplementary Fig. 3c.

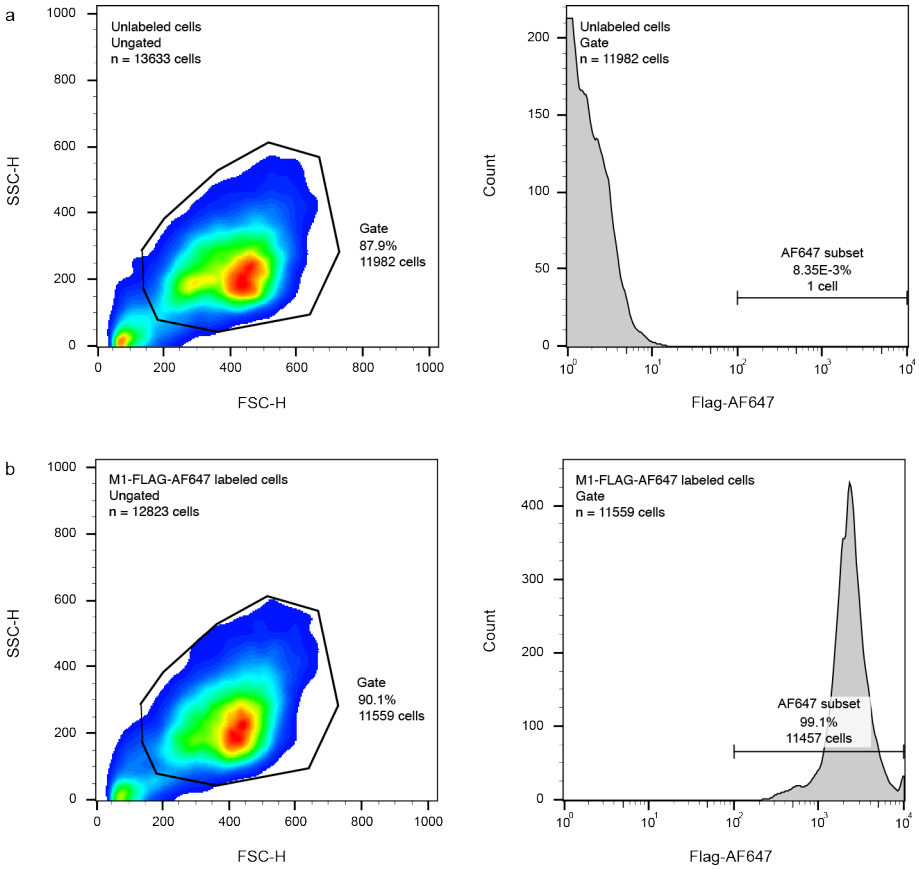

Supplementary Figure 5. Gating strategy for flow cytometry experiments to calculate β2AR internalization. Gating strategy applied to **a**, unlabeled cells and **b**, M1-FLAG-AF647 labeled cells.

Variable	Reported value	Reference
D of GFP	~30 $\mu m^2 s^{-1}$	Swaminathan et al. 1997
D of GFP	24 $\mu m^2 s^{-1}$	Potma et al. 2001
D of PKAcat	4.4 $\mu m^2 s^{-1}$	Li et al. 2015
k_{on}	5 x 10^6 $M^{-1}s^{-1}$	Cheng et al. 2001
k_{on}	5 x 10^5 $M^{-1}s^{-1}$	Zawadzki et al. 2004
[PKAreg]	2 x 10^{-6} M	Walker-Gray et al. 2017
[PKAcat]	2 x 10^{-7} M	Walker-Gray et al. 2017
k_{on}*	1-10 s^{-1}	k_{on}* = k_{on} x [PKAreg]

Supplementary Table 1. Table of known values of GFP and PKA for estimating lifetime (t) and displacement (x) in Supplementary Table 2.

D ($\mu m^2 s^{-1}$)	**k_{on}*** (s^{-1})	**t** (s)	**x** (μm)
30	10	0.1	3.46
24	10	0.1	3.1
4.4	10	0.1	1.33
30	1	1	10.95
24	1	1	9.8
4.4	1	1	4.2

Supplementary Table 2. Estimation of PKAcat distance traveled before rebinding PKAreg based on diffusion coefficients, on rates and concentrations from Supplementary Table 1. Time constant for reassociation, t, defined by 1/k_{on}*. Distance, x, before rebinding is calculated from $x = \sqrt{4Dt}$.

Locus	sgRNA guide sequence	Insert	Donor DNA
PRKACA	TAATACGACTCACTATAGGC GGCCGCCGCCGCCGCGATG TTTAAGAGCTATGCTGGAA	$mNG2_{11}$	GGGGCCGCCGGCCGCAGCCAGCACCCGCCG CGCCGCAGCTCCGGGACCGGCCCCGGCCGCC GCCGCCGCGATG**ACCGAGCTCAACTTCAAGG AGTGGCAAAAGGCCTTTACCGATATGATG**GGT GGCGGCGGCAACGCCGCCGCCGCCAAGAAGG GCAGCGAGCAGGAGAGCGGTGAGTGCCCGGG CTGTGACCCCGATC
PRKACA	TAATACGACTCACTATAGGC GGCCGCCGCCGCCGCGATG TTTAAGAGCTATGCTGGAA	GFP_{11}	GGGGCCGCCGGCCGCAGCCAGCACCCGCCG CGCCGCAGCTCCGGGACCGGCCCCGGCCGCC GCCGCCGCGATG**CGTGACCACATGGTCCTTC ATGAGTATGTAAATGCTGCTGGGATTACA**GGT GGCGGCGGCAACGCCGCCGCCGCCAAGAAGG GCAGCGAGCAGGAGAGCGGTGAGTGCCCGGG CTGTGACCCCGATC

Supplementary Table 3. List of DNA sequences used for knock-in cell line generation.

Cell line	Outer Forward Primer	Outer Reverse Primer	Insert Forward	Insert Reverse
PRKACA-$mNG2_{11}$	CGCGAGCGAGTGAAT GGCCGAGAGTCCGCG GTGCGTGTCCCGAGG CTGAGAGCCTATAGT	TAGGCAGAGAGGATG AGGGGCCCCGTAGG GGGAGGGGCCAGGC GATGATGGACAA	ACCGAGCTCAACT TCAAGGAGTGGCA AAAGGCCTTTACC GATATGATGGGTG GCGGC	GCCGCCACCCATC ATATCGGTAAAGG CCTTTTGCCACTCC TTGAAGTTGAGCTC GGT
PRKACA-GFP_{11}	CGCGAGCGAGTGAAT GGCCGAGAGTCCGCG GTGCGTGTCCCGAGG CTGAGAGCCTATAGT	TAGGCAGAGAGGATG AGGGGCCCCGTAGG GGGAGGGGCCAGGC GATGATGGACAA	CGTGACCACATGG TCCTTCATGAGTAT GTAAATGCTGCTG GGATTACAGGTGG CGGC	GCCGCCACCTGTA ATCCCAGCAGCAT TTACATACTCATGA AGGACCATGTGGT CACG

Supplementary Table 4. List of PCR primers for knock-in cell line validation.

Primer	Sequence
GAPDH forward	CTGCCCAAGATCTTCCATGT
GAPDH reverse	GACAAGCTTCCCGTTCTCAG
PCK1 forward	CTGCCCAAGATCTTCCATGT
PCK1 reverse	CAGCACCCTGGAGTTCTCTC
CHC17 forward	ACTTAGCCGGTGCTGAAGAA
CHC17 reverse	AACCGACGGATAGTGTCTGG

Supplementary Table 5. List of qRT-PCR primers.

Antibody	Manufacturer	Catalog #	Dilution
Rabbit anti PKAcat α (C-20)	Santa Cruz Biotechnology	sc-903	1:1000
Rabbit anti PKAreg IIα (C-20)	Santa Cruz Biotechnology	sc-908	1:1000
Mouse anti PKAreg IIβ Clone 45	BD Biosciences	610625	1:1000
Mouse anti Giantin [9B6]	Abcam	ab37266	1:1000
Sheep anti TGN46	Bio-Rad	AHP500GT	1:1000
Mouse anti EEA1 Clone 14	BD Biosciences	610457	1:1000
Donkey anti Mouse AlexaFluor 647	Invitrogen	A31571	1:500
Goat anti Rabbit AlexaFluor 647	Invitrogen	A21245	1:500
Donkey anti Sheep AlexaFluor 555	Invitrogen	A21436	1:500

Supplementary Table 6. List of antibodies used for immunofluorescence.

Antibody	Manufacturer	Catalog #	Dilution
Mouse anti CREB (86B10)	Cell Signaling Technologies	9104	1:2000
Rabbit anti pCREB (S133) (87G3)	Cell Signaling Technologies	9198	1:2000
Rabbit anti PKA C-α	Cell Signaling Technologies	4782	1:2000
Mouse anti HDAC2 (3F3)	Cell Signaling Technologies	5113	1:2000
Mouse anti α-tubulin (DM1A)	Cell Signaling Technologies	3873	1:10000
IRDye 680RD Donkey anti-Mouse IgG	LI-COR Biosciences	926-68072	1:10000
IRDye 800CW Donkey anti-Rabbit IgG	LI-COR Biosciences	926-32213	1:10000

Supplementary Table 7. List of antibodies used for western blots.

Supplementary References

1. Swaminathan, R., Hoang, C. P. & Verkman, A. S. Photobleaching recovery and anisotropy decay of green fluorescent protein GFP-S65T in solution and cells: cytoplasmic viscosity probed by green fluorescent protein translational and rotational diffusion. *Biophys. J.* **72**, 1900–1907 (1997).
2. Potma, E. O. *et al.* Reduced protein diffusion rate by cytoskeleton in vegetative and polarized Dictyostelium cells. *Biophys. J.* **81**, 2010–2019 (2001).
3. Li, L., Gervasi, N. & Girault, J.-A. Dendritic geometry shapes neuronal cAMP signalling to the nucleus. *Nat. Commun.* **6**, 6319 (2015).
4. Cheng, X., Phelps, C. & Taylor, S. S. Differential binding of cAMP-dependent protein kinase regulatory subunit isoforms Ialpha and IIbeta to the catalytic subunit. *J. Biol. Chem.* **276**, 4102–8 (2001).
5. Zawadzki, K. M. & Taylor, S. S. cAMP-dependent protein kinase regulatory subunit type IIbeta: active site mutations define an isoform-specific network for allosteric signaling by cAMP. *J. Biol. Chem.* **279**, 7029–36 (2004).
6. Walker-Gray, R., Stengel, F. & Gold, M. G. Mechanisms for restraining cAMP-dependent protein kinase revealed by subunit quantitation and cross-linking approaches. *Proc. Natl. Acad. Sci.* **114**, 10414–10419 (2017).